Symmetric and Asymmetric Coalescence of Drops on a Substrate

J. F. Hernández-Sánchez, L. A. Lubbers, A. Eddi, and J. H. Snoeijer

Physics of Fluids Group, MESA+Institute for Nanotechnology, J. M. Burgers Centre for Fluid Dynamics, University of Twente, P. O. Box 217, 7500 AE Enschede, The Netherlands

(Received 10 July 2012; revised manuscript received 8 August 2012; published 2 November 2012)

The coalescence of viscous drops on a substrate is studied experimentally and theoretically. We consider cases where the drops can have different contact angles, leading to a very asymmetric coalescence process. Side view experiments reveal that the "bridge" connecting the drops evolves with self-similar dynamics, providing a new perspective on the coalescence of sessile drops. We show that the universal shape of the bridge is accurately described by similarity solutions of the one-dimensional lubrication equation. Our theory predicts that, once the drops are connected on a microscopic scale, the bridge grows linearly in time with a strong dependence on the contact angles. Without any adjustable parameters, we find quantitative agreement with all experiments.

DOI: 10.1103/PhysRevLett.109.184502 PACS numbers: 47.55.D−, 47.85.mf

The coalescence or breakup of liquid drops is a fundamental process relevant for the formation of raindrops or sprays, inkjet printing, or stability of foams and emulsions [1–4]. The initial stages of coalescence of two spherical drops has been characterized in great detail [5–10]. After contact, a small liquid bridge connects the two drops and the bridge grows rapidly with time. Depending on the viscosity of the liquid, the radius of the bridge grows as $r \sim t$ (high viscosity) [5–8], or $r \sim t^{1/2}$ (low viscosity, inertia dominated) [7–9], with a crossover depending on fluid properties and drop size [10].

In many cases, however, the coalescing drops are not freely suspended but are in contact with a substrate. Much less is known about the coalescence of such sessile drops. When looking from a top view, the coalescence of drops on a substrate looks very similar to the case for spherical drops [Fig. 1(d)]; yet the bridge dynamics is fundamentally different. Measurements of the top view width of the bridge r for very viscous drops give a growth $r \sim t^{1/2}$ [11,12], and even smaller exponents have been suggested [13]. The challenge lies in the complications introduced by the presence of the substrate. First, the geometry of the drop is no longer a sphere with an axisymmetric bridge, but a spherical cap with a contact angle θ. As a consequence, a top view of the coalescence process is very different from a side view. Second, the wall slows down the liquid transport towards the bridge [11] and gives rise to the motion of a contact line [14]. At present, it is not clear whether or not this contact line motion affects the initial stages of coalescence, and different predictions for the θ dependence have been reported [11–13]. Based on numerical simulations it was argued that the main flow direction is parallel to the wall and oriented towards the bridge [11], as sketched in Fig. 1(d). While this simplifies the description of the coalescence, this hypothesis remains to be validated experimentally.

In this Letter we resolve the coalescence of viscous drops on a substrate by performing side view experiments, imaging parallel to the substrate (Fig. 1). Our central finding is that, once the contact is established on a nanometer scale, the bridge develops a self-similar shape and its height grows linearly as $h_0 \sim t$. The influence of the contact angle is studied in detail by considering drops with identical or different contact angles, resulting in symmetric or asymmetric coalescence [Figs. 1(b) and 1(c)]. Theoretically, we show that all experiments are described quantitatively by a one-dimensional lubrication theory. We identify similarity solutions that quantitatively predict the shape and evolution of the bridge without adjustable

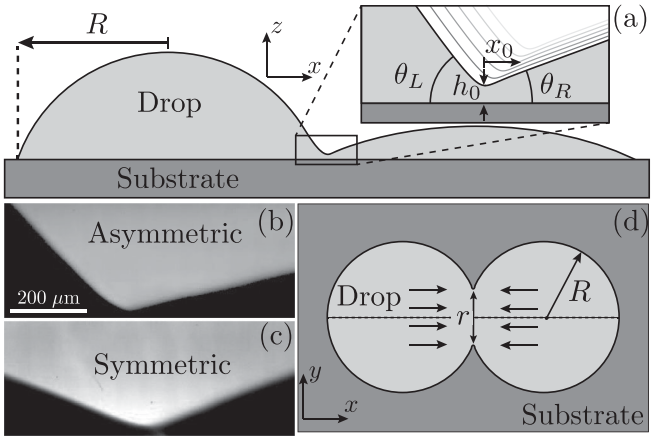

FIG. 1. (a) Schematic of two coalescing viscous drops on a substrate, viewed from the side. The minimum height $h_0(t)$ characterizes the bridge height. The left-right contact angles θ_L and θ_R can be different at the moment of contact. The horizontal displacement x_0 results from the asymmetry in the contact angles. (b), (c) Typical frames of the experiments are shown for asymmetric contact angles (b) and symmetric contact angles (c). (d) Schematic of two coalescing viscous drops, viewed from the top. The lubrication model assumes that the flow is parallel to the solid wall and predominantly in the x direction (arrows) [11]. The width of the bridge is $r(t)$.

parameters. This confirms the hypothesis by Ristenpart *et al.* [11] that the coalescence is governed by liquid flux from the drop into the bridge. Our results reveal that the rate of vertical growth scales with the contact angle as $\sim\theta^4$, the horizontal speed $\sim\theta^3$, and provide a new perspective on previous top view measurements.

Experimental setup.—The side view images of coalescing drops in Figs. 1(b) and 1(c) are obtained by a digital video camera (Photron APX-RS) equipped with a microscopic lens (Navitar 12x zoom lens), resulting in a resolution of 2 μm/pixel. The camera recorded 12.5 frames per second. The substrate consists of a horizontal microscope glass slide (Menzel precleaned microscope slide, average roughness $\approx$ 10 nm). The glass slide was further cleaned using ethanol and acetone, then submerged in an ultrasonic bath and dried with filtered nitrogen gas. The coalescing drops were made from silicon oils (Basildon Chemical Company Limited), with viscosity $\eta = 0.974$ Pa $\cdot$ s or 12.2 Pa $\cdot$ s, which both have a surface tension $\gamma = 21 \times 10^{-3}$ N $\cdot$ m^{-1} and density $\rho = 975$ kg $\cdot$ m^{-3}. The silicon oils perfectly wet the cleaned glass slide ($\theta_{\mathrm{eq}} \approx 0$).

The coalescence of two drops is controlled as follows. A first drop is deposited from the syringe on the substrate. Although the silicon oil perfectly wets the glass, the spreading of these high viscosity drops is very slow, with the liquid contact angle decreasing slowly in time. Subsequently, the glass plate is displaced by a manual translation stage and a second drop is placed next to the first one. By controlling the volume of silicon oil and the time between the deposition of drops we achieve a range of contact angles θ_L and θ_R between 10° to 67° at the time of coalescence. We consider both symmetric coalescence [$\theta_L = \theta_R$, Fig. 1(c)] and asymmetric coalescence [$\theta_L \neq \theta_R$, Fig. 1(b)]. The spreading determines the initial conditions, but in all cases the spreading speed is much smaller than the growth of the bridge. We verified that the weak spreading does not influence our results by performing some experiments under partially wetting conditions, for which the coalescence was started from equilibrium. Contact time is determined when there is a visual change, which happens before the bridge is thick enough to provide a reliable measurement. The dashed line in Fig. 2(a) shows this spatial resolution limit.

Self-similar dynamics.—The dynamics of coalescence is characterized by the growth of the bridge connecting the two drops. Figure 2(a) presents the height of the bridge h_0 defined in Fig. 1, as a function of time for a symmetric coalescence experiment ($\theta_L = \theta_R = 22°$). At early times, we observe a linear increase of the bridge height, i.e., $h_0 \sim t$, while at later times the coalescence slows down. In these final stages the height of the bridge becomes comparable to the total drop size, which is typically $\sim$1 mm for all experiments. The very early stage, however, exhibits self-similar dynamics that is governed by a single length scale. This is revealed in Fig. 2(b) where the

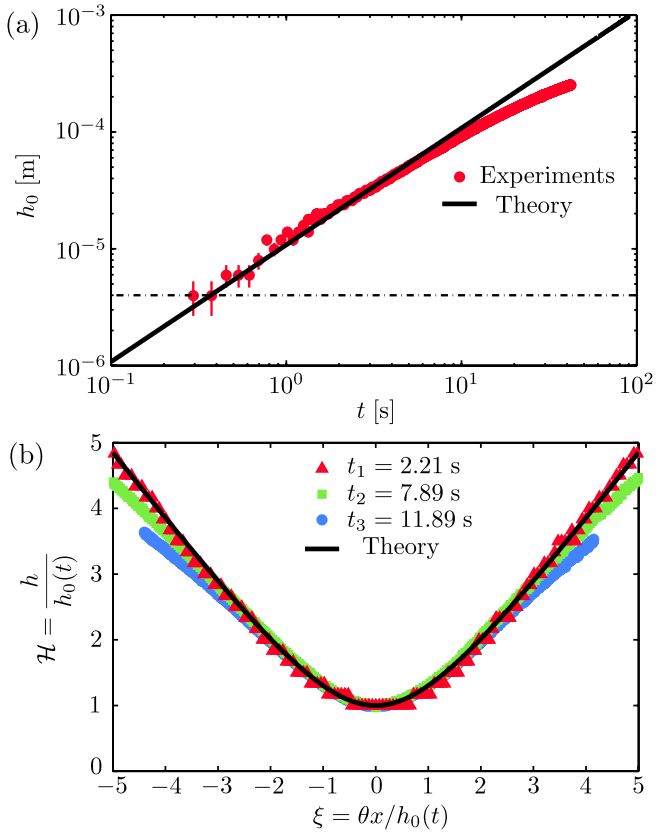

FIG. 2 (color online). Symmetric coalescence. (a) Height of the bridge h_0 as a function of time after contact t, for drops with $\theta_L = \theta_R = 22°$ ($\eta = 12.2$ Pa $\cdot$ s). Experiments are shown in red (●), the solid line is the prediction by Eqs. (2) and (3). The dashed line represents the lower limit for spatial resolution. (b) Rescaled experimental profiles at different times, $\mathcal{H} = h(x,t)/h_0(t)$ versus $\xi = x\theta/h_0(t)$. The collapse reveals self-similar dynamics at the early stage of coalescence, in agreement with the similarity solution (solid line).

meniscus profiles, $h(x,t)$, and the horizontal coordinate, x, are rescaled by $h_0(t)$. The scaled profiles at different times collapse onto a universal curve: the early stages of coalescence are characterized by a self-similar meniscus profile. The size of the bridge is simply h_0, both in the horizontal and vertical direction. The solid line is the theoretical similarity profile that will be derived below.

Our experiments suggest that coalescence of drops on a substrate is governed by a similarity solution of the flow. To simplify the three-dimensional geometry of the coalescence, we assume that the flow is predominantly along the wall and oriented as sketched in Fig. 1(d), as suggested by Ristenpart *et al.* [11]. We therefore attempt a similarity solution based on the one-dimensional lubrication theory for viscous flows [15]:

$$\frac{\partial h}{\partial t} + \frac{\gamma}{3\eta}\frac{\partial}{\partial x}\left(h^3\frac{\partial^3 h}{\partial x^3}\right) = 0. \qquad (1)$$

Here, $h(x, t)$ is the meniscus profile viewed from the side, η is the liquid viscosity and γ denotes the surface tension. This lubrication equation is valid for small contact angles and represents mass conservation: the second term is the surface tension-driven flux of liquid towards the bridge, causing a growth of the bridge ($\partial h/\partial t > 0$). A direct comparison with side view experiments will test the validity of the one-dimensional assumption.

Consistent with our experiments, Eq. (1) has a similarity solution that imposes a linear time dependence,

$$h(x, t) = vt\mathcal{H}(\xi), \quad \text{with} \quad \xi = \frac{\theta x}{vt}, \tag{2}$$

where $\mathcal{H}(\xi)$ is the similarity profile of the meniscus bridge. Here we incorporated the contact angle θ in the scaling of x, such that the condition $\partial h/\partial x = \theta$ translates to $\mathcal{H}' = 1$. The correct scaling of the coalescence velocity with θ then turns out to be

$$v = V\frac{\gamma\theta^4}{3\eta}, \tag{3}$$

where V is a numerical constant that still needs to be determined. In combination with (1) and (2), this provides an ordinary differential equation (ODE) for the similarity profile $\mathcal{H}(\xi)$:

$$\mathcal{H} - \xi\mathcal{H}' + \frac{1}{V}(\mathcal{H}^3\mathcal{H}''')' = 0. \tag{4}$$

In order to solve Eq. (4), which is a fourth order ODE with one unknown parameter V, five boundary conditions are required. At the center of the symmetric bridge

$$\mathcal{H}(0) = 1, \quad \mathcal{H}'(0) = \mathcal{H}'''(0) = 0, \tag{5}$$

while far away the profile has to match a linear slope of contact angle θ. For the similarity variables this becomes

$$\mathcal{H}''(\infty) = 0, \qquad \mathcal{H}'(\infty) = 1. \tag{6}$$

The boundary value problem (4)–(6) uniquely determines the similarity solution for symmetric drop coalescence. It was solved numerically using a shooting algorithm, from which we obtained both the dimensionless velocity, $V = 0.818\,809$, and the similarity profile $\mathcal{H}(\xi)$. As the influence of the contact angle was scaled out, the solution describes the coalescence for all contact angles, within the lubrication assumption of small θ.

The similarity solution indeed provides an accurate description of the coalescence experiments. The solid line in Fig. 2(a) is the prediction (3) without adjustable parameters. The solid line in Fig. 2(b) is the similarity profile $\mathcal{H}(\xi)$ obtained from our analysis. The agreement between experiment and theory shows that the coalescence dynamics is accurately described by a one-dimensional lubrication model. As expected, the similarity solution breaks down at later times when the size of the meniscus bridge becomes comparable to the size of the drops.

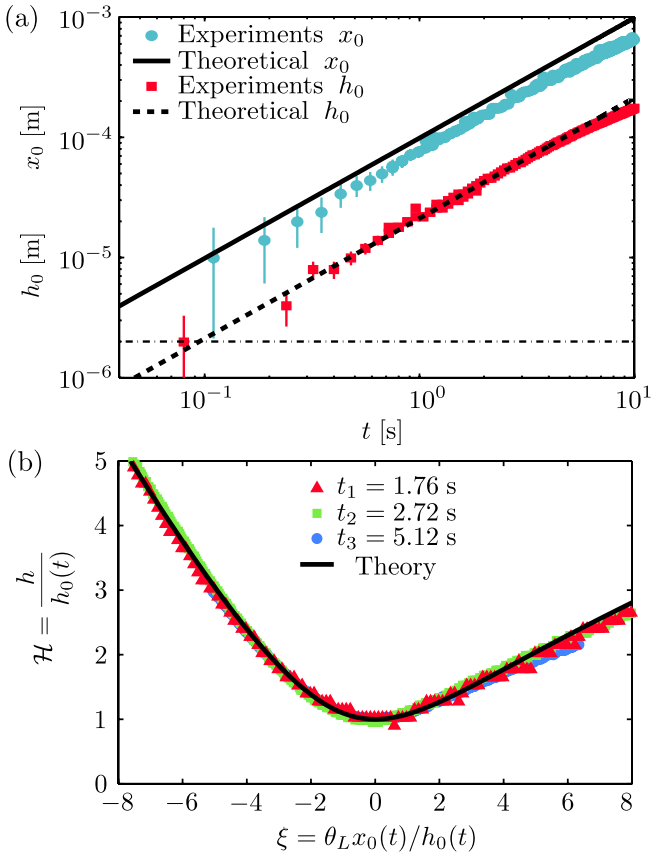

FIG. 3 (color online). Asymmetric coalescence. (a) Horizontal and vertical position of the meniscus bridge, $x_0(t)$ and $h_0(t)$, for asymmetric drops ($\theta_L = 46°$, $\theta_R = 13°$, viscosity $\eta = 12.2$ Pa · s). Blue (●) and red (■) markers are experimental data for x_0 and h_0, respectively. Solid and dashed lines are the predictions from the similarity solutions. (b) Rescaled experimental profiles at different times, $\mathcal{H} = h(x, t)/h_0(t)$ versus $\xi = x_0\theta_L/h_0(t)$. The collapse reveals self-similar dynamics at the early stage of coalescence. The solid line is the similarity solution predicted by our analysis.

Similarly, a cutoff for the scale-free solution will appear when h falls within the range of molecular interactions. Details on how contact is established initially are beyond the similarity solution and will depend on nanoscopic features such as the presence of a precursor film [16,17].

Asymmetric coalescence.—We further extend the theory to asymmetric coalescence, for which the contact angles $\theta_L \neq \theta_R$ (Fig 1). Without loss of generality, we assume that $\theta_L > \theta_R$, and scale the coordinates using θ_L. Interestingly, the lack of symmetry induces a *horizontal* displacement of the meniscus bridge during the coalescence process: the minimum of the bridge, x_0, is pulled towards the lower contact angle (θ_R). This effect can be captured using a similarity variable that is comoving with the bridge, of the form

$$\xi = \frac{\theta_L(x - ut)}{vt}, \quad \text{with} \quad u = U\frac{\gamma\theta_L^3}{3\eta}. \tag{7}$$

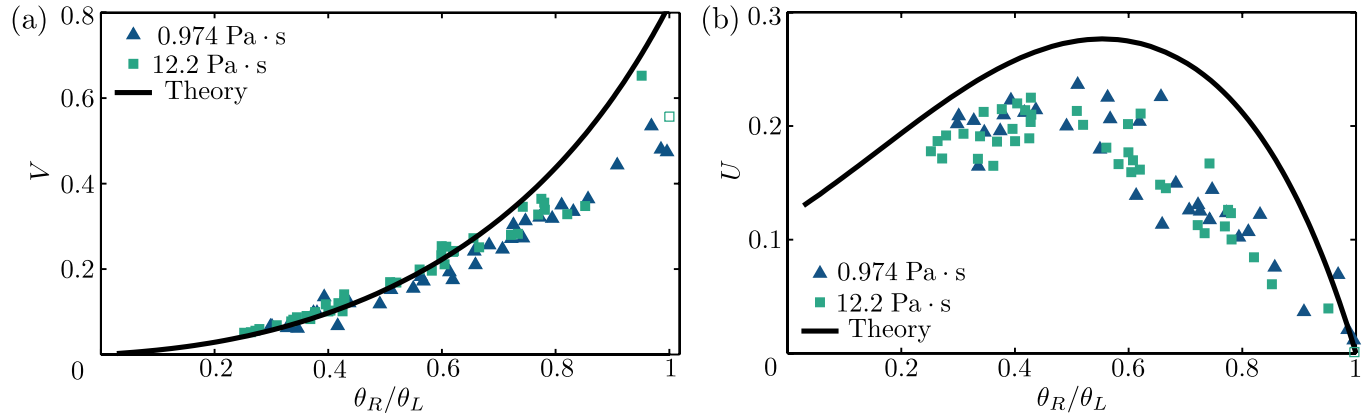

FIG. 4 (color online). Contact angle dependence of coalescence velocity. (a) Dimensionless vertical speed, $V = 3v\eta/(\gamma\theta_L^4)$, as a function of θ_R/θ_L. (b) Dimensionless horizontal speed, $U = 3u\eta/(\gamma\theta_L^3)$, as a function of θ_R/θ_L. The horizontal speed vanishes for the symmetric case $\theta_R/\theta_L = 1$, and displays a maximum around $\theta_L/\theta_R \sim 0.5$. Closed symbols: 75 experiments on completely wetting substrate. Open symbols: drops on partially wetting substrate ($\theta_{eq} = 55°$). Solid lines: similarity solutions.

The horizontal velocity of coalescence u scales with θ_L^3, where U is a numerical constant. The vertical velocity still follows (3) with $\theta = \theta_L$. Inserting (7) into (1) yields

$$\mathcal{H} - \left(\xi + \frac{U}{V}\right)\mathcal{H}' + \frac{1}{V}(\mathcal{H}^3\mathcal{H}''')' = 0. \qquad (8)$$

This fourth order ODE for $\mathcal{H}(\xi)$ now contains two unknown parameters U and V; hence, the solution requires six boundary conditions. The minimum of the bridge is still defined by $\mathcal{H}(0) = 1$, $\mathcal{H}'(0) = 0$, but the symmetry condition on $\mathcal{H}'''$ no longer applies. Instead, one has to impose $\mathcal{H}''(-\infty) = \mathcal{H}''(\infty) = 0$, with contact angles

$$\mathcal{H}'(-\infty) = -1, \qquad \mathcal{H}'(\infty) = \theta_R/\theta_L. \qquad (9)$$

The resulting boundary value problem has a unique solution for each ratio θ_R/θ_L, selecting both U and V.

Figure 3 compares theory and experiment for an asymmetric coalescence ($\theta_R/\theta_L = 0.25$). The horizontal position of the bridge x_0 (blue circles) and the vertical position of the bridge h_0 (red squares) are shown in Fig. 3(a). These again evolve linearly in time with a well-defined velocity. The solid and dashed lines are the predictions (3) and (7), with prefactors U and V determined from the similarity solution. Figure 3(b) confirms that the asymmetric experimental profiles indeed display self-similarity (symbols), in excellent agreement with theory (solid line).

We finally consider the influence of the contact angle on the coalescence speed. Our theory suggests a universal behavior when making the horizontal and vertical velocities dimensionless, according to $U = 3u\eta/(\gamma\theta_L^3)$ and $V = 3v\eta/(\gamma\theta_L^4)$. The results of 75 experiments are summarized in Fig. 4 and compared to the theoretical prediction. Indeed, we observe a good collapse of the data. The open symbol corresponds to a case where the substrate is partially wetting. The agreement with the (slowly) spreading drops shows that the initial coalescence is governed by the bridge geometry, not by the substrate wettability. An interesting feature is that the theory predicts an optimal horizontal speed around $\theta_R/\theta_L \approx 0.5$, which is verified experimentally. This maximum horizontal velocity can be explained as follows. The asymmetry induces a bias in the pulling force of surface tension, which is more efficient for the smaller contact angle θ_R. However, the "lubrication effect" inhibits liquid transport when $\theta_R \to 0$, as the viscous friction in the liquid increases for smaller angles. The combination of these two effects gives rise to an optimum ratio θ_R/θ_L.

Discussion.—Our results imply that the coalescence of drops on a substrate, which is manifestly three dimensional, is described quantitatively by a one-dimensional model. This can be explained from the cross section of the bridge perpendicular to our viewpoint, r, which is much larger than h_0 [Fig. 1]. Elementary geometry suggests $r \sim (Rh_0/\theta)^{1/2}$ [12], R being the footprint radius of the drop on the substrate. At early times we therefore have $r \gg h_0$, such that local gradients will be oriented in the x direction. This is consistent with numerical characterization of the flow field [11]. It would be interesting to see whether the one-dimensional approach also applies for coalescence of low-viscosity drops, which are dominated by inertia rather than viscosity [2,18].

Our findings also highlight the key importance of asymmetry on the coalescence dynamics. While here the asymmetry is due to the contact angles, a similar effect was found for merging drops with unequal surface tensions (such as water and alcohol), for which the coalescence is strongly delayed by Marangoni forces [19]. This will have a strong bearing on applications such as inkjet printing, for which such asymmetries are encountered naturally due to spreading and evaporation of ink drops.

We thank K. Winkels and S. Huisman for discussions. This work is sponsored by Lam Research, STW and NWO by VIDI Grant No. 11304.

[1] J. Eggers, Rev. Mod. Phys. **69**, 865 (1997).
[2] N. Kapur and P. H. Gaskell, Phys. Rev. E **75**, 056315 (2007).
[3] C. Andrieu, D. Beysens, V. S. Nikolayev, and Y. Pomeau, J. Fluid Mech. **453**, 427 (2002).
[4] M. P. Brenner, X. D. Shi, and S. R. Nagel, Phys. Rev. Lett. **73**, 3391 (1994).
[5] J. Eggers, J. R. Lister, and H. A. Stone, J. Fluid Mech. **401**, 293 (1999).
[6] R. W. Hopper, J. Fluid Mech. **213**, 349 (1990).
[7] S. T. Thoroddsen, K. Takehara, and T. G. Etoh, J. Fluid Mech. **527**, 85 (2005).
[8] D. G. A. L. Aarts, H. N. W. Lekkerkerker, Hua Guo, G. H. Wegdam, and D. Bonn, Phys. Rev. Lett. **95**, 164503 (2005).
[9] L. Duchemin, J. Eggers, and C. Josserand, J. Fluid Mech. **487**, 167 (2003).
[10] J. D. Paulsen, J. C. Burton, and S. R. Nagel, Phys. Rev. Lett. **106**, 114501 (2011).
[11] W. D. Ristenpart, P. M. McCalla, R. V. Roy, and H. A. Stone, Phys. Rev. Lett. **97**, 064501 (2006).
[12] R. D. Narhe, D. A. Beysens, and Y Pomeau, Europhys. Lett. **81**, 46 002 (2008).
[13] M. W. Lee, D. K. Kang, S. S. Yoon, and A. L. Yarin, Langmuir **28**, 3791 (2012).
[14] D. Bonn, J. Eggers, J. Indekeu, J. Meunier, and E. Rolley, Rev. Mod. Phys. **81**, 739 (2009).
[15] A. Oron, S. H. Davis, and S. G. Bankoff, Rev. Mod. Phys. **69**, 931 (1997).
[16] M. L. Forcada and C. M. Mate, Nature (London) **363**, 527 (1993).
[17] H. P. Kavehpour, B. Ovryn, and G. H. McKinley, Phys. Rev. Lett. **91**, 196104 (2003).
[18] J. Billingham and A. C. King, J. Fluid Mech. **533**, 193 (2005).
[19] S. Karpitschka and H. Riegler, Langmuir **26**, 11 823 (2010).